Astrophysics, Vol. 53, No. 4, 2010

CIRCUMNUCLEAR DENSE GAS IN OH-MEGAMASER GALAXIES

R. A. Kandalyan[1,2] and M. M. Al-Zyout[2]

The properties of a sample of extragalactic OH maser sources over a wide spectral range are discussed. Based on a sample of 22 maser galaxies it is shown that OH, HCN, and x-ray emission are closely related. On the other hand, these emissions depend on the mass of the galactic nucleus. It is shown that the broadening of the OH emission line is caused by the rotation of the circumnuclear disk, dense regions of which serve as the sources of OH and HCN emission. X-ray heating can excite OH and HCN molecules.

Keywords: *masers- galaxies: molecules- galaxies: x-ray emission*

1. Introduction

The HCN molecule has a large dipole moment ($\mu \sim 2.98D$), so its emission at $\lambda \sim 3.4$ mm (J=1-0) originates in dense layers of molecular gas ($n_{H2} \geq 10^4$) within the circumnuclear region of galaxies (< 1 kpc) and maps ("traces") the dense gas regions [1,2]. It is known that megamaser OH and x-ray emission also originate in the circumnuclear region of galaxies. Thus, there is some interest in studying the interrelation of these three radiations, as well as their connection with the mass of galactic nuclei.

It has been found [3] that the relative fraction of dense gas is high ($L_{HCN}/L_{CO} > 0.07$) in OH megamasers. However, the number of galaxies with HCN emission examined in that paper [3] was not large, only 8. At present (May 2010) the number of HCN megamasers is roughly a factor of two larger. In addition, we are interested in the interrelationship between the emission by OH and HCN molecules and the mass of galactic nuclei and in the role of x-ray emission in dense gas regions. This paper is a first attempt to examine these questions in OH megamasers.

(1) V. A. Ambartsumyan Byurakan Astrophysical Observatory, Armenia; e-mail: kandalyan@yahoo.com kandalyan@aabu.edu.jo
(2) Institute of Astronomy and Space Sciences, Al-Beit University, Jordan

Original article submitted May 24, 2010; accepted for publication September 8, 2010. Translated from Astrofizika, Vol. 53, No. 4, pp. 529-537 (November 2010).

0571-7256/10/5304-0475

Our analysis is based on nonparametric statistical methods, which provide a more correct analysis of the observational data, especially when the sample size is small and possible selection effects must be taken into account [4]. In section 2 we discuss the sample of megamasers. The Spearman nonparametric correlation technique is introduced in section 3. The results of the analysis are presented in section 4. These results are discussed in section 5.

2. The sample of OH megamasers

At present, about 120 megamasers are known [5-10]. Of this number, we have selected those galaxies for which either emission of HCN molecules has been detected or the mass of the nucleus is known. The number of such galaxies is 22 (Table 1). Table 1 lists the following, in sequence: (1) galaxy name, (2) red shift z, (3) width (FWHM)

TABLE 1. List of the 22 OH Megamasers

IRAS	z	W (km/s)	$\log L_{OH}$ ($L_\odot$)	$\log L_{2\text{-}10}$ (erg/s)	$\log L_{HCN}$ (K km s^{-1} pc^2)	$\log M_c$ ($M_\odot$)	Refs.
00509+1225	0.061	410	2.31			7.26	[14]
01418+1651	0.027	110	2.75	40.48		6.85	[15]
09320+6134	0.039	120	1.80	41.68	9.00		
10173+0828	0.048	39	2.41	39.15		6.90	[16]
11010+4107	0.035	200	2.09	40.67	8.60		
11257+5850	0.010	246	1.18	41.37	8.32		
11506-3851	0.011	120	1.50		8.50		
12071-0444	0.128	233	2.68	41.12		7.46	[17]
12112+0305	0.073	280	3.11	41.20	9.03		
12243-0036	0.007	70	-0.14	39.25	7.65		
12540+5708	0.042	290	2.87	42.43	9.27	8.95	[18]
13428+5608	0.038	141	2.60	42.36	9.18	8.18	[19]
15065-1107	0.006	102	-0.18		6.96		
15107+0724	0.013	150	1.03		8.15		
15327+2340	0.018	117	2.49	40.91	8.96	7.08	[20]
16300+1558	0.242	130	2.87			7.52	[17]
17208-0014	0.042	164	2.99	41.33	9.58	8.37	[16]
20550+1656	0.036	112	2.05		8.35		
22025+4205	0.014	152	0.62		8.24		
22491-1808	0.077	171	2.49	40.88		7.42	[17]
23234+0946	0.128	263	2.63			7.39	[17]
23365+3604	0.064	299	2.77	41.50	9.18	7.57	[16]

W of the line in the rest system of the galaxy, km/s, (4) luminosity of maser emission, L_{OH}, in solar units, and (5) x-ray luminosity over 2-10 keV, $L_{2\text{-}10\text{keV}}$, in erg/s. The x-ray data are taken from Ref. 11. Column 6 lists the HCN luminosity L_{HCN} in *K* km s^{-1} pc^2. This unusual unit for the luminosity L_{HCN} is related to the peculiar features of spectral observations in the millimeter range, where the line intensity is often expressed as an integral of the brightness temperature with respect to the emission velosity [12]. The HCN observation data were taken from Refs. 1, 2, and 13. Column (7) is the mass M_c of the assumed black hole in solar units, for which the references are given in column (8). The luminosity of the HCN molecule was calculated using the equation [12]

$$L_{HCN} = 3.25 \cdot 10^7 \cdot S_{HCN} \cdot \Delta V \cdot \nu^{-2} \cdot D_L^2 \cdot (1+z)^{-3},$$

where $S_{HCN} \cdot \Delta V$ is the integral flux in Jy·km·s^{-1}, ν is the observed line frequency in GHz, D_L is the distance in Mpc, and *z* is the red shift. The luminosities L_{OH} and $L_{2\text{-}10\text{keV}}$, and D_L were calculated using equations given in Ref. 21. The Hubble constant was taken to be $H_o = 75$ km/s/Mpc.

3. The Spearman rank correlation and partial correlation coefficients

One of the ways of estimating the correlation coefficient between two variables is Spearman's nonparametric technique [22]. Rather than the values *x* and *y* of the variables, themselves, in this method their ranks are used (order number, when the variables are arranged in increasing order). The Spearman rank-order correlation coefficient is given by

$$\rho = \frac{\sum_{i=1}^{n} \left(R_{x_i} - \overline{R}_x\right)\left(R_{y_i} - \overline{R}_y\right)}{\sqrt{\sum_{i=1}^{n} \left(R_{x_i} - \overline{R}_x\right)^2 \cdot \sum_{i=1}^{n} \left(R_{y_i} - \overline{R}_y\right)^2}},$$

where R_{x_i} and R_{y_i} are the ranks of the *i*-th element of the variables *x* and *y*, respectively. $\overline{R}_x = \frac{1}{n}\sum_{i=1}^{n} R_{x_i}$ and $\overline{R}_y = \frac{1}{n}\sum_{i=1}^{n} R_{y_i}$ are the mean values of the ranks of the variables *x* and *y*, respectively. For large *n* ($n > 10$), the Spearman coefficient has a Student's *t*-distribution, $(n-2)^{1/2}\rho / \left(1-\rho^2\right)^{1/2}$.

We now proceed to the partial correlation coefficients. Suppose we have three random variables *x, y*, and *z* which are mutually correlated. We are interested in the correlation coefficient between the variables *x* and *y*, with the variable *z* fixed. In other words, we want to calculate a "partial" correlation coefficient between *x* and *y*, subtracting the correlation between *x* and *z*, on one hand, and between *y* and *z*, on the other. This type of correlation is known as a partial correlation coefficient and is defined as follows:

$$\rho_{xy.z} = \frac{\rho_{xy} - \rho_{xz}\rho_{yz}}{\sqrt{\left(1-\rho_{xz}^2\right)\left(1-\rho_{yz}^2\right)}},$$

where $\rho_{xy.z}$ is the partial correlation coefficient between x and y with the variable z fixed, ρ_{xy}, ρ_{xz}, and ρ_{yz} are the correlation coefficients between the corresponding variables. The distribution of the partial correlation coefficients also obeys a Student's t-distribution: $(n-4)^{1/2}\rho/\left(1-\rho^2\right)^{1/2}$. Anomalous values of random variables do not affect the Spearman rank-order coefficients, so that, when a sample of data is nonuniform and sparse, a nonparametric method is to be preferred over the Pearson parametric method.

4. Analysis of results

According to Kolmogorov-Smirnov statistics, almost all the parameters listed in Table 1 have distributions that are not normal. Thus, in the case of our sample of megamasers, the use of nonparametric regression and correlations techniques is fully justified [4]. To begin with, we calculated the Spearman correlation coefficients between the parameters listed in Table 1, including the red shift. In those cases where the variables of a given pair also depend on the red shift (the so-called Malmqvist effect), we used the Spearman partial correlation coefficients in order to eliminate the Malmqvist effect from the given correlation. Following this analysis, we selected those pairs of variables which have significant correlation coefficients (by significant correlation we mean a probability of a random correlation between the variables $P \le 0.05$).

Table 2 lists the results of the statistical analysis, with the most significant Spearman partial correlations ρ (taking the Malmqvist effect into account) indicated. Pairs of variables for which the Spearman correlation coefficients are of little significance are not listed in Table 2. The table lists the results of a linear Kendall-Theil regression [4] (slope S; intersection point I; 95% confidence interval for the slope, and median deviation d). If the median deviation d is close to zero, then the linear regression is a suitable approximation. In Table 2, $\log L_{\rm OH}$, $\log L_{\rm HCN}$, and $\log L_{\rm 2\text{-}10keV}$ are dependent variables, while the others are independent. In particular, the regression line between $\log L_{\rm OH}$ and $\log L_{\rm HCN}$ is given by

$$\log L_{\rm OH} = 1.54 \log L_{\rm HCN} - 11.23.$$

We have examined the dependence of the maser emission parameters ($L_{\rm OH}$ and W) on the x-ray emission previously. (See Ref. 11 and the references therein.)

5. Discussion

As noted above, in megamaser galaxies, the maser, x-ray, and HCN emissions are produced in the circumnuclear

TABLE 2. Correlation and Regression Coefficients

	$\log M_c$	$\log L_{\rm HCN}$
$\log L_{\rm OH}$	N = 12 $\rho = 0.62$ P = 0.03 S = 0.26 I = 0.73 $0.03 \le S \le 0.53$ d = -0.04	N = 15 $\rho = 0.85$ P = 2 10^{-4} S = 1.54 I = -11.23 $1.02 \le S \le 1.97$ d = -0.3
$\log L_{\rm HCN}$	$\log W$ N = 15 $\rho = 0.57$ P = 0.03 S = 2.35 I = 3.49 $0.42 \le S \le 4.73$ d = – 0.13	$\log L_{\rm 2\text{-}10keV}$ N = 10 $\rho = 0.65$ P = 0.04 S = 0.36 I = - 5.89 $0.05 \le S \le 0.79$ d = – 0.13
$\log L_{\rm 2\text{-}10keV}$	$\log M_c$ N = 9 $\rho = 0.92$ $P = 5 \cdot 10^{-4}$ S = 1.27 I = 31.68 $0.55 \le S \le 1.95$ d = 0	

region. Thus, it might be expected that these emissions should depend on one another; in addition, they may depend on the mass of the galactic nucleus. The mass of the nucleus can be estimated assuming that an accretion disk and a presumed black hole are at the center of the galaxy. Unfortunately, other assumptions regarding galactic nuclei do not yield an estimate of the mass of the nucleus. Figure 1 is a plot of $\log L_{\rm OH}$ *vs.* $\log M_c$ for the megamasers, with the Kendall-Theil regression line indicated. Figure 2 is a plot of $\log L_{\rm OH}$ *vs.* $\log L_{HCN}$ with the Kendall-Theil regression line indicated. This dependence is very close and the spread in the points relative to the regression line is not large (see Table 2, as well). The results of Table 2 and Ref. 11 show clearly that the different indicators of dense gas (L_{OH}, L_{HCN}) in the circumnuclear region of megamasers are closely coupled and that they, in turn, depend on the x-ray emission and the mass of the nucleus. We now examine the interrelation between the x-ray emission and the mass of the galactic nuclei. According to Table 2,

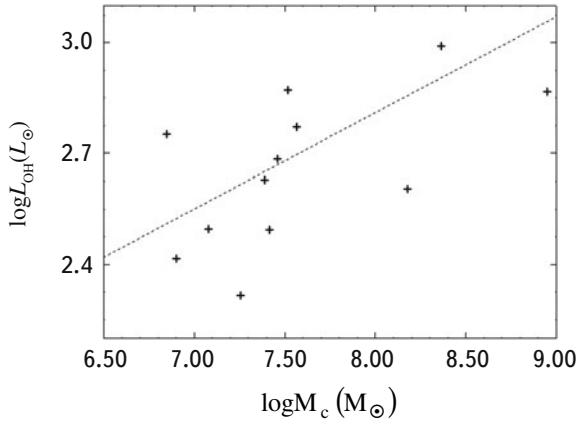

Fig. 1. Relation between megamaser emission and the mass of the galactic nucleus. The Kendall-Theil regression line is shown (see Table 2).

$$\log L_{2-10\mathrm{keV}} = 1.27 \log M_c + 31.68 .$$

In Ref. 11 we showed that $L_{2-10\mathrm{keV}} = kW^S$, where $k = 10^{35.53}$ and $S = 2.56$. In addition, if we assume that the line width W in megamasers is primarily determined by the Kepler rotation of the circumnuclear disk, we find that $W \sim (GM_c/R)^{1/2}$ [23], where G is the gravitational constant and R is the disk radius. Therefore, these last two formulas imply that $L_{2-10\mathrm{keV}} \sim k(GM_c/R)^{S/2}$, or $L_{2-10\mathrm{keV}} \sim M_c^{2.56/2} = M_c^{1.28}$. It is surprising that these entirely different methods of calculating the slope of $L_{2\text{-}10\mathrm{keV}}$ as a function of M_c yield essentially the same result (1.27 and 1.28). Furthermore, Eq. (2) of Ref. 23 can be used to calculate the expected widths of the lines for the four galaxies, for which the required parameters of their rotating disks have been measured by *VLBI* observations. The results of these calculations are shown in Table 3, which lists W_{calc} (the calculated line width), W_{obs} (the observed line width according to the *VLBI* data), and references to the *VLBI* observations and disk parameters. It is clear that the calculated and

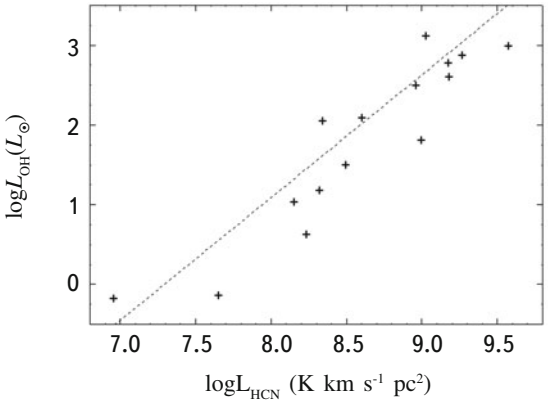

Fig. 2. Relation between the megamaser and HCN luminosities. The Kendall-Theil regression line is shown (see Table 2).

TABLE 3. Calculated and Observed OH Line Widths

Designation	W_{calc} (km/s)	W_{obs} (km/s)	Refs.
IRAS 01418+1651III Zw 35	39	30-40	[15,24]
IRAS 12540+5708 Mkn 231	216	214	[18,25]
IRAS 13428+5608 Mkn 273	132	141	[19]
IRAS 15327+2340 Arp 220	27	20-40	[20,26]

observed line widths are in good agreement.

The above analysis, together with the results listed in Tables 2 and 3, indicate, first of all, that the line width of the OH emission is determined by the rotation of the circumnuclear disk. Second, the OH and HCN molecular emissions and the x-ray emission are interrelated. It is also interesting that L_{HCN} and $L_{2\text{-}10\mathrm{keV}}$ depend on the width of the OH line (L_{OH} depends on W by definition, since the intensity of the OH emission is the flux integrated with respect to velocity), which characterizes the velocity field of the rotating disk, although the HCN and x-ray emissions come from spatially different components of the circumnuclear region. *HCN* and OH represent the molecular part of the disk, and the x-rays, the high temperature plasma lying closer to the center of the galaxy. It is possible that the x-ray emission somehow excites the HCN and OH emission lines, for example, through x-ray heating of a circumnuclear molecular cloud [27]. In that case, we might expect the molecular and x-ray emissions to be related. We believe that this question requires detailed study.

6. Conclusion

We have studied a sample of extragalactic OH maser sources over a wide spectral range. In our analysis we used a nonparametric linear regression and correlation technique. We summarize the major results of this paper as follows: (1) the OH, HCN, and x-ray emissions are closely coupled to one another. On the other hand, they depend on the mass of the galactic nucleus. (2) The line width of the OH emission is determined by the rotation of the circumnuclear disk of a galaxy, within dense layers of which OH and HCN molecules exist. It is possible that x-ray emission excites the line emission from the OH and HCN molecules.

REFERENCES

1. Y. Gao and P. M. Solomon, Astrophys. J. Suppl. Ser. **152**, 63 (2004).
2. Y. Gao and P. M. Solomon, Astrophys. J. **606**, 271 (2004).
3. J. Darling, Astrophys. J. **669**, L9 (2007).
4. R. A. Kandalyan and M. M. Al-Zyout, Astrofizika **53**, 363 (2010).
5. J. -M. Martin, PhD thesis, University de Paris VII, France (1989).

6. J. -M. Martin, L. Bottinelli, M. Dennefeld, et al., C. R. Acad. Sci. Paris, **308**(II), 287 (1989).
7. L. Stavely-Smith, R. P. Norris, J. M. Chapman, et al., Mon. Notic. Roy. Astron. Soc. **258**, 725 (1992).
8. W. A. Baan, J. J. Salzer, and R. D. LeWinter, Astrophys. J. **509**, 633 (1998).
9. J. Darling and R. Giovanelli, Astron. J. **124**, 100 (2002).
10. M. X. Fernandez, E. Momjian, C. J. Salter, and T. Ghosh, Astron. J. **139** (2066 (2010).
11 R. A. Kandalyan, V. V. Hambaryan, and H. A. Sabat, Astrofizika **50**, 171 (2007).
12. P. M. Solomon, D. Downes, S. J. E. Radford, and J. W. Barrett, Astrophys. J. **478**, 144 (1997).
13. W. A. Baan, C. Henkel, A. F. Loenen, A. Baudry, and T. Wiklind, Astron. Astrophys. **477**, 747 (2008).
14. M. Vestergaard, Astrophys. J. **571**, 733 (2002).
15. Y. M. Pihlstrom, J. E. Conway, R. S. Booth, P. J. Diamond, and A. G. Polatidis, Astron. Astrophys. **377**, 413 (2001).
16. N. Murray, E. Quataert, and T. A. Thompson, Astrophys. J. **618**, 569 (2005).
17. K. M. Dasyra, L. J. Tacconi, R. I. Davies, et al., Astrophys. J. **638**, 745 (2006).
18. A. M. S. Richards, R. J. Cohen, G. H. Cole, et al., in "Galaxies and their Constituents at the Highest Angular Resolutions", Proceedings of IAU Symp. 205 (2001), ed. R. T. Schilizzi, (Manchester, UK), p. 212.
19. J. A. Yates, A. M. S. Richards, M. M. Wright, et al., Mon. Notic. Roy. Astron. Soc. **317**, 28 (2000).
20. E. Rovilos, P. J. Diamond, C. J. Lonsdale, C. J. Lonsdale, and H. E. Smith, Mon. Notic. Roy. Astron. Soc. **342**, 373 (2003).
21. R. A. Kandalyan, Astron. Astrophys. **404**, 513 (2003).
22. W. L. Conover, *Practical Non-parametric Statistics*, 2nd Ed., New York, John Wiley and Sons (1980).
23. R. A. Kandalyan, Astrofizika **48**, 421 (2005).
24. A. S. Trotter, J. M. Moran, L. J. Greenhill, X. Zheng, and C. R. Gwinn, Astrophys. J. **485**, L79 (1997).
25. H. R. Klockner, W. A. Baan, and M. A. Garrett, Nature, **421**, 821 (2003).
26. C. J. Lonsdale, P. J. Diamond, H. E. Smith, and C. J. Lonsdale, Astrophys. J. **493**, L13 (1998).
27. D. A. Neufeld, P. R. Maloney, and S. Conger, Astrophys. J. **436**, L127 (1994).